Journal of the Korean Institute of Electrical and Electronic Material Engineers. Vol. 12, No. 11, pp. 1007-1018, 1999.

Conduction Mechanism Analysis and Oscillation Phenomena of Low Voltage ZnO Varistor

논 문
12-11-4

Kyung-Uk Jang*, Myung-Ho Kim*, Woo-Heon Park***, Joon-Ung Lee**

Abstract

ZnO varistors have an excellent non-linearity and a large surge-energy absorption capability. For these reasons, the ZnO varistors are widely used to protect electrical/electronic circuits from an abnormal surge and/or noise signal. In order to obtain the low-voltage varistor with randomly distributed large seed grain within bulk, the ZnO varistors are made by a new three-composition seed grain method. From the I-V characteristics of the fabricated varistors, the knee voltage of varistors with the seed grain 5wt% is 5 V. We may also present a carrier oscillation properties for the low-voltage varistor fabricated by the new method of three-composition seed grain.

Key Words(중요용어) : ZnO varistor, Low voltage varistor, Seed grain, 3-composition seed grain, I-V characteristics

1. INTRODUCTION

ZnO varistors are nonlinear devices which are commonly used for a suppression of transient pulses and surges in electronic devices or power lines[1].

The current-voltage (I-V) characteristic of varistor is strongly nonlinear. At low voltage, varistor is highly resistive more than 10^{10} Ω-cm, while at the high electric field the current acrossing the varistor can be very large as described by the empirical equation[2]

$$I = (KV)^{\alpha} \quad (1)$$

where, K is geometric constant of sample, α a nonlinear coefficient. The nonlinear coefficient of ZnO varistor shows up to above α 50. A knee voltage of the varistor can be generally written as[3]

$$V = N_g \cdot V_g \quad (2)$$

where, N_g is the numbers of ZnO grains in series within the sample and V_g the knee voltage per grain boundary. Therefore, the microstructure of low voltage ZnO varistor has to be fairly large size of grain in order to obtain the low voltage varistor[4].

In this paper, it is introduced that a distribution of large grain size in ZnO for low voltage varistor is due to discontinuous grain growth and can be narrowed by using a 3-composition seed grain method. We also present the fact that the conduction mechanism of the fabricated varistor can be divided into the three region. The conduction properties of varistor, which was measured in the temperature range of 30~120℃ with the current range of 10^{-8}~10^{2}A/㎠, was divided into the three region having different conduction mechanisms as the current was increased : The region I (say, leakage-current region) in E_{int} ⟨ 25 MV/m shows an

* : Kyungwon College, San 65, Bokjung-dong, Soojong-gu, Songnam-shi, Korea
** : Next President of KIEEME
*** : NARA ENGINEERING CONSULTANT
1999년 1월 29일 접수, 1999년 9월 17일 심사완료

Ohmic conduction. The region Ⅱ (say, pre-breakdown region) in the 25 < E_{int} < 70 MV/m can be explained by the Poole-Frenkel and Schottky conduction mechanism, and the region Ⅲ (breakdown region) in E_{int} 70 MV/m is dominated by the tunneling effect.

The oscillation phenomena of carriers in current-voltage characteristics below the knee voltage are explained by the transient flow of nontrapped carriers group in the trap level of intergranular layer, surface state and/or depletion layer[5].

In particular, the current oscillation phenomena are hardly shown in the high electric field. It is why that the injected carriers from both electrodes are directly transported from the conduction band of forward biased ZnO grain into the reverse biased ZnO grain through the intergranular layer, since the trap level in the electric field above the knee voltage is mostly filled.

2. EXPERIMENT

Fine powder composed with ZnO(97 mol%), $BaCO_3$(2.5 mol%) and TiO_2(0.5 mol%) were pressed at 450 kg/cm², and sintered in the furnace at 1400 ℃ for 10 hrs.

After those processes, the sintered bodies were washed in the boiled water, and then four kinds of different seed grain were obtained.

The compounds mixed with ZnO(98 mol%), Bi_2O_3(1 mol%), CoO(0.5 mol%) and MnO_2(0.5 mol%), of which the seed grain contents are 0, 5, 10, 20 and 40 wt%, were pressed at 450 kg /cm². The pressed bodies were sintered in the furnace at 1300 ℃ for 2 hrs. Then the sintered bodies were polished with silicon carbide abrasive of 1200 meshes into the thickness of 1.0 mm. The contacts were done with the silver paste to the surface of sample for 12 mm in diameter and 1 mm in thickness. The fabrication procedure of sample is given in Fig. 1.

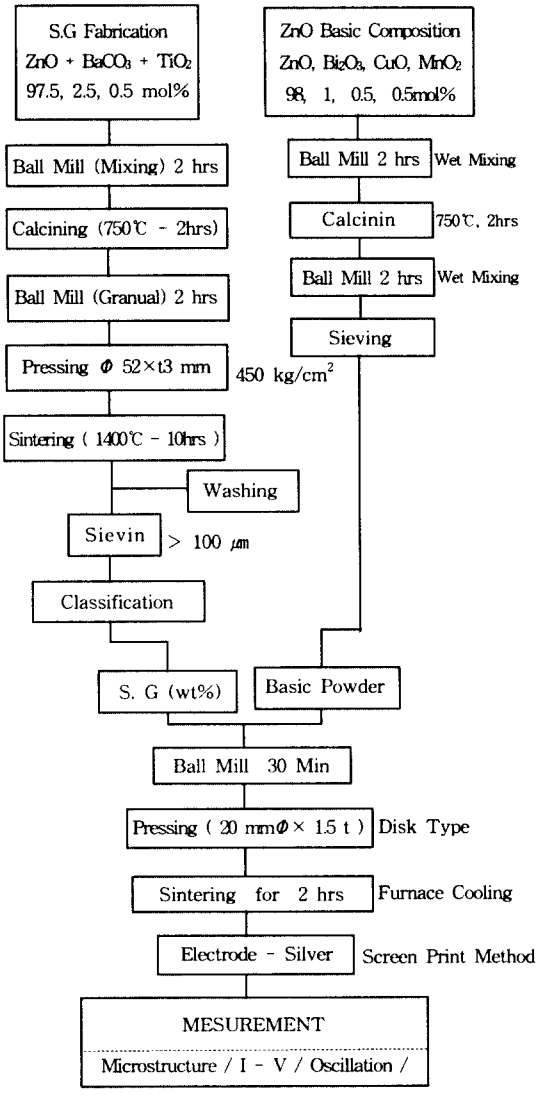

Fig. 1. The fabrication procedure of sample.

Electrical measurement of the sample was performed in the current range from 10^{-8} to 10^{2} A/cm² within the temperature range from 30 to 120 ℃, as shown in Fig. 2.

The carrier oscillation measurement of sample was performed with the amplifier (NF Electronic Instrument bx-31, USA), power supply(Keithley 237, USA) and oscilloscope(Yokogawa PL 2140B, JAPAN), as

shown in Fig. 3.

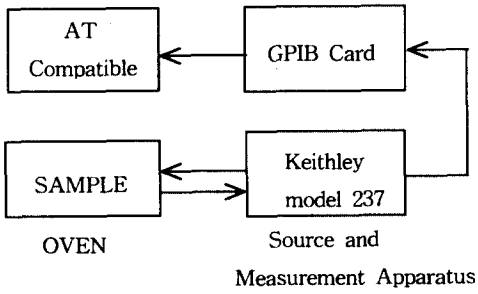

Fig. 2. Block diagram for I-V measuring apparatuses.

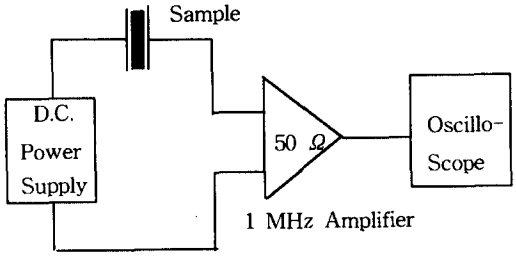

Fig. 3. Measurement of oscillation phenomena.

3. RESULTS AND DISCUSSION

Fig. 4 shows the current-voltage characteristics of the samples with the various contents of seed grain, and Fig. 5 suggests the nonlinear coefficient α was decreased from 30 to 11. The values of α may largely depend on the existence of intinsic pore and a third phase in the sample[6, 11]. Fig. 6 shown the knee voltage of ZnO varistor as a function of seed grain contents. It can be concluded from the microstructure of the samples that the phenomena are considered by a corelation between the different grain sizes of base powder and the seed grains as well as the different radius of curvature.

The pore and the secondary recrystalline in the sample seem to grow due to increase

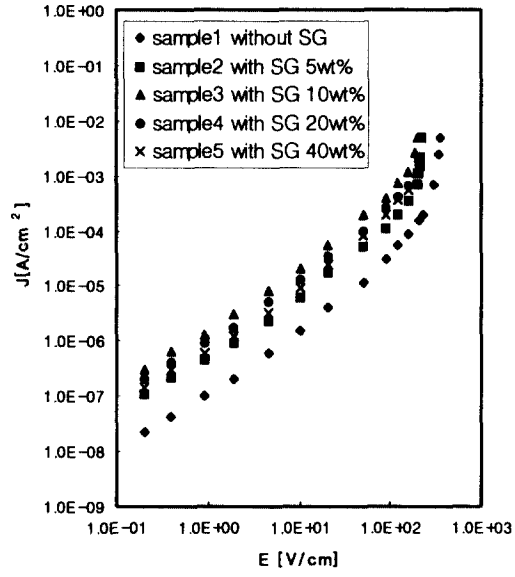

Fig. 4. Current-Voltage characteristics of ZnO varistor with the contents of the seed grain.

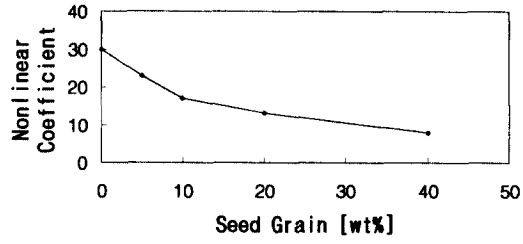

Fig. 5. Nonlinear coefficient of ZnO varistor as a function of the seed grain content.

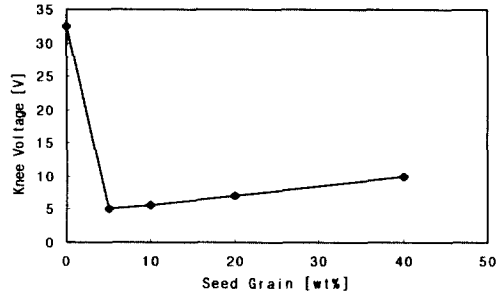

Fig. 6. Knee voltage of ZnO varistor as a function of the seed grain content.

in the seed grain content. The mean size of seed grain is increased by secondary recrystallization during sintering. The optimized content rate of seed grain in the sample was 5 wt %.

The conduction mechanism of low-votage varistor with 5 wt% content of seed grain was classified by the three regions with different mechanism as shown in Fig. 7.

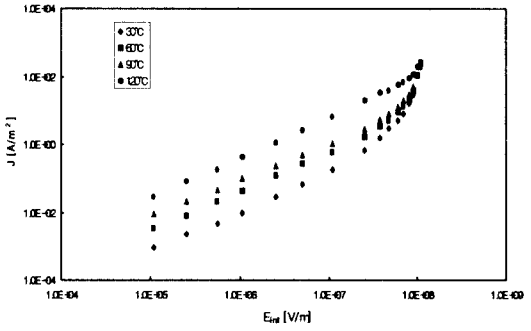

Fig. 7. Current-voltage characteristics of ZnO varistor with the content of seed grain 5 wt% for several different measuring temperatures.

Fig. 7 show the temperature dependent current-voltage characterictics of the specimen added 5wt% of seed grain. As seen in the Fig. 7, the knee voltage is $5V_{(1mA/cm^2)}/mm$, and the temperature dependence is relatively large at low electric-field region, but hardly seen at about high electric-field region. The knee voltage of varistor is depended on the breakdown voltage of intergranular layer and the number of its[3]. In Fig. 7, when the thickness of specimen is 1 mm and the size of grain is tens of μm, it is not describe that the knee voltage of specimen is $5V_{(1mA/cm^2)}/mm$. If the large seed grain was added in the specimen, these results could be explained by the large seed grain with low resistivity distributed randomly, which is conduction path, because the knee voltage is independent on the effective mean size of seed grain and ZnO grain[6]. When the specimen added seed grain is sintered, the knee voltage of varistor is lowered because the grain size is depended on the secondary growth during the large seed grain and raw ZnO powder is sintered[7]. It is known that the current is increased as the temperature of the specimen is increased, and also the current density is linearly proportional to the strength of the electric field.

The current density increases nonlinearly at the transition region above the low-electric field. It is considered that the current density increases due to the electron injected from electrode according to the increment of temperature. And then, we also know that the rapid-varying region in I-V characteristics is not affected by the measured temperature at all.

Therefore, we explain I-V characteristics with three regions according to conduction process in order to represent the conduction mechanism of varistor added 3-composition seed grain. First, the leakage-current region, that is, the low current ohmic region A, the nonlinear conduction region B and the the breakdown region C of varistor appear sequentially. Also, so as to analyze the above conduction mechanisms, we must consider the electric field Eint instead of the electric field applied specimen because the depletion layer really acts as an insulator[8]. So, we obtained Eint from the depletion layer thickness of 200Å calculated in the result of C-f characteristics[12].

As known from Fig. 7, the nonlinear coefficient α and its temperature dependence are different in prebreakdown and brekdown region. Therefore, the electrical conduction mechanism of the low-voltage ZnO varistor can't be decribed with one conduction mechanism. So, we could analyze the 3 region in Fig. 7 with 3 conduction mechanisms.

(1) Contuction mechanism

The conduction current depends on the temperature and electric stress. Results of measurements are given in Fig. 7, which shows the conduction current of the ZnO varistor at constant temperature(30 and 120 ℃) as a function of the electric field stress.

The relationship between conduction current and electric field is not linear, i.e., nonohmic. Three different regions, region Ⅰ, Ⅱ, and Ⅲ, may be distinguished in the diagram[8]. Region Ⅰ is below 25 MV/m, region Ⅱ is in between 25 MV/m and 70 MV/m, and region Ⅲ is above 70 MV/m.

1) Leakage current region, E_{int} < 25 MV/m

Leakage current is important factor in causing the degradation of varistor, because it always flows before operation of varistor.

The Ohmic conduction mechanism in ZnO varistor has been studied by many researchers[6]. L. M. Levinson found that in the Ohmic region of conduction of ZnO varistor the diffusion current generally may be disregarded because it is such a small value[8].

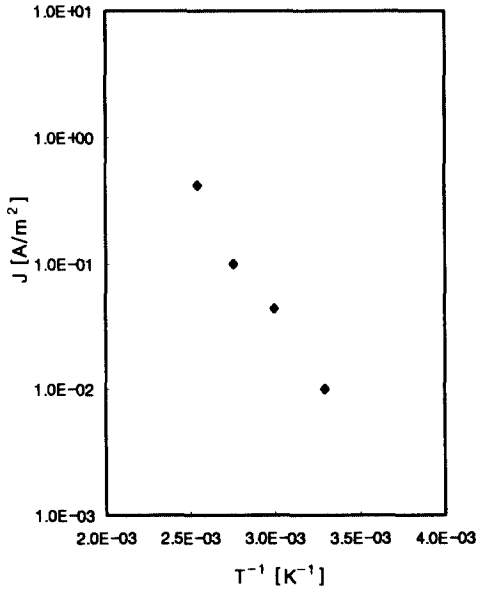

Fig. 8. Plot of log J vs. reciprocal temperature in region Ⅰ.

Our results in region Ⅰ, electric field stress below 25MV/m, support the Ohmic conduction mechanism theory.

Fig. 8 is the Arrhenius plots of log J at steady state vs. 1/T for region Ⅰ of Fig. 7. The activation energy obtained from the diagram is 0.36eV. Similar values have been obtained by other workers.

The carriers attributed to the conduction current may be due to ionic impurities. The carriers of impurities may be formed in the intergranular layers during the fabrication process.

2) Prebreakdown region, 25 < E_{int} < 70 MV/m

Various theories were proposed by many researchers in the conduction mechanism of region Ⅱ[1, 3]. In Fig. 7, prebreakdown region (region Ⅱ) is analyzed by the Poole-Frenkel emission theory considering the extrinsic level or trap between intergranular layers, because it has larger dependence of the electrical field than the leakage current region. Fig. 9 was obtained from Fig. 7, and shows the linear relationship between the log σ and $E^{\frac{1}{2}}$.

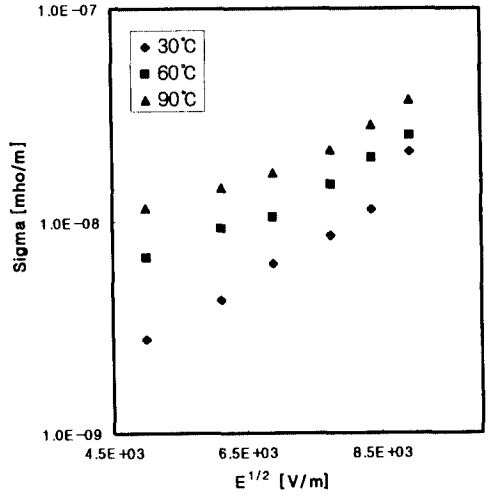

Fig. 9. Plot of log σ vs. $E^{\frac{1}{2}}$ in region Ⅱ.

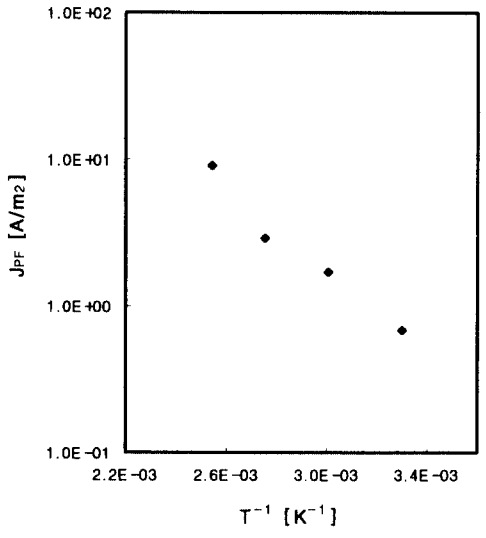

Fig. 10. Plot of J_{PF} vs. reciprocal temperature in Poole-Frenkel region.

Thus Poole-Frenkel or Schottky conduction mechanisms may be operative in this region. Charge injected from a metal and ZnO grain to the intergranular layer of insulator at medium fields may takes place by field-assisted thermionic emission, a process known as Schottky emission. The force exerted on a particle at a distance x from the interface is given by

$$F = eE - \frac{e^2}{4\pi\varepsilon_o\varepsilon_r(2x)^2} \tag{3}$$

The work done on the particle is

$$W = -\int f dx = -eEx + \frac{e^2}{4\pi\varepsilon_o\varepsilon_r}4x + \varphi \tag{4}$$

The constant of integration has been chosen so that W $\equiv \phi$ at a large distance from the electrode under zero applied field. For nonzero field, W has a maximum value ϕ_{app} at the point where F=0. This gives the result

$$\phi_{app} = \phi - \beta_s E^{\frac{1}{2}} \quad \beta_S = \left(\frac{e^3}{4\pi\varepsilon_o\varepsilon_r}\right)^{\frac{1}{2}} \tag{5}$$

Consequently, the current density drawn over this barrier is

$$J_s = A\,T^2 \exp\left(-\frac{\phi}{kT}\right)\exp\left(\frac{e^3}{4\pi\varepsilon_o\varepsilon_r}\right) \tag{6}$$

Where A = $12\times10^5[A/m^2\,k^2]$, ϕ is the potential barrier, ε_r is the dielectric constant at high frequency, and T is the absolute temperature. When electric field interacts with the coulombic potential barrier of the trap, the height of the barrier is lowered. This process known as the Poole-Frenkel effect is the bulk analogous of the Schottky effect at an interfacial barrier. Since the potential energy of an electron in a coulombic field, $-e^2/4\pi\varepsilon_o\varepsilon_r$, is four times that due to image force effects. The Poole-Frenkel attenuation of a coulombic barrier, ϕ_{PF}, in a uniform electric field is twice that due to the Schottky effect at a neutral barrier

$$\Delta\phi_{PF} = \left(\frac{e^3}{\pi\varepsilon_o\varepsilon_r}\right)^{\frac{1}{2}} E^{\frac{1}{2}} = \beta_{PF}E^{\frac{1}{2}} \tag{7}$$

$$\beta_{PF} = \left(\frac{e^3}{\pi\varepsilon_o\varepsilon_R}\right)^{\frac{1}{2}}$$

Thus, the conductivity is field-dependent and the current density drawn over this barrier is

$$J_{PF} = J_O\exp\left(-\frac{\phi}{2kT}\right)\exp\left(\frac{\beta_{PF}E^{\frac{1}{2}}}{2kT}\right) \tag{8}$$

To determine whether it is Poole-Frenkel or Schottky process, the slope of the straight lines in Fig. 9 are compared with the theoretically calculated slopes β_{th} from the Schottky relationship : $\beta_s = (e^3/4\pi\varepsilon_o\varepsilon_r)^{\frac{1}{2}}$.

In our sample, the theoretical value (β_{th}) of β_s 1.56×10^{-24}. If the value of β obtained from the slope is close to that of β_{th} obtained theoretically, the process is that of Schottky emission.

If the value of β obtained from the slope is double that of β_{th}, the process is that of Poole-Frenkel emission. From the slope of straight line in Fig. 9, we found that β_{PF} is 3.4×10^{-24} and ε_r is 13, respectively.

The Arrhenius plot for a field of 44MV/m is shown in Fig. 10. The barrier height value is Φ = 0.7 eV.

In our study, the value of β_{PF} is double that of the theoretically calculated $\beta_{th}(1.56\times10^{-24})$ and $\beta_s(1.68\times10^{-24})$ which was obtained in the end part of region Ⅱ (E_{int} between 50~70MV/m) ;

$\beta_{PF}=3.4\times10^{-24}\fallingdotseq2\times1.56\times10^{-24}(2\ \beta_{th})\fallingdotseq2\times1.68\times10^{-24}(2\beta_s)$. Therefore, the conduction mechanism in region Ⅱ is likely to be dominated by the Poole-Frenkel effect. In this region, either the Poole-Frenkel or Schottky conduction mechanism may be operative as in region Ⅱ, and shows the relationship of straight line between the log σ and $E^{\frac{1}{2}}$. The slope β_s obtained in this region is close to β_{th} (1.56×10^{-24}) calculated theoretically, and equal to half the slope $\beta_{PF}(3.4\times10^{-24})$ for the Poole-Frenkel effect.

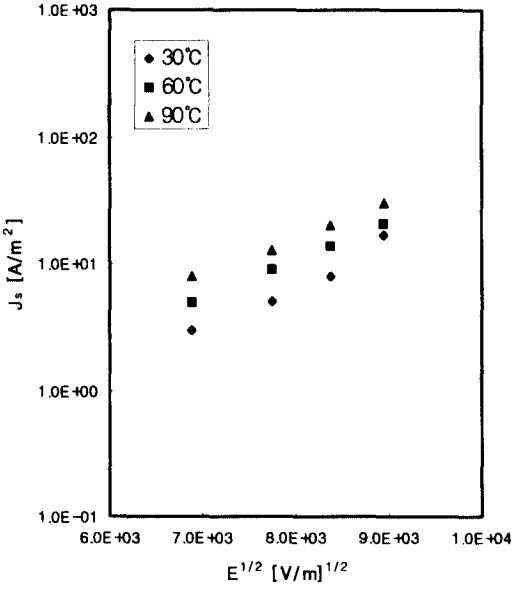

Fig. 11. Plot of log J_s vs. $E^{\frac{1}{2}}$ in region Ⅱ.

The donor level, Φ, the potential barrier between the metal contact and dielectric material is obtained from the relationship of $\log(J_s/T^2)$ vs. 1/T at the applied field of 60MV/m(Fig. 12). The donor level obtained is Φ =0.24 eV at an applied field of 60MV/m in Schottky region.

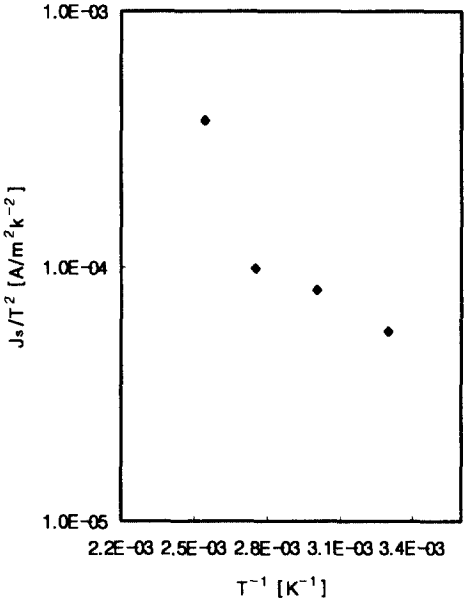

Fig. 12. Plot of log J_s vs. reciprocal temperature.

3) Breakdown region, E_{int} > 70 MV/m

The conduction mechanism of breakdown region independenting on the ambient temperature has been proposed several theories so far, that is, space charge limited current, schottky emission theory and electron avalanche theory and so on. But these theories are not efficiently explained the experimental phenomena in that region. Therefore, we apply the tunnel theory to the breakdown region. The magnitude of the knee voltage is considered with Fowler-Nordheim tunneling effect from the relation between the microstructure and equivalent circuit of the sample.

The increase in conduction current in region Ⅲ (Fig. 7) is larger than expected

from the Schottky effect in region Ⅱ. At very high fields in the ZnO varistor, the potential barrier becomes very thin and a different mechanism comes into play. Electrons injected into intergranular layer from the electrode and ZnO grain pass through thin potential barriers despite of having insufficient energy to surmount them ; this is known as tunneling. When this occurs at the interface barrier it is known as Fowler-Nordheim injection where the current is

$$J_{FN}=A_1E^2\exp(-B/E) \quad (9)$$

where $A_1 = 2.2\ e_2/8\pi h\psi$ and $B_2=-8\pi d(2m)^{\frac{1}{2}}\ \psi^{3/2}/3he$, m is effective electron mass and h is Plank constant. Fig. 13 shows the $\log(J_{FN}/E^2)$ vs. 1/E plot, and from the slope the potential barrier $\Phi=0.3$ eV was obtained. Generally, the tunneling current depends strongly on the applied field and is independent of temperature[5, 9]. However, in our experimental results the tunneling current slightly depends on temperature because the carriers first penetrate from the metal electrode into potential barrier and then the penetrated carriers are released by thermal excitation into the conduction band of ZnO. Both thermionic and field emission occur simultaneously.

The barrier height in each region may be dominated by the electric field and temperature.

Therefore, the conduction mechanism in each region is different.

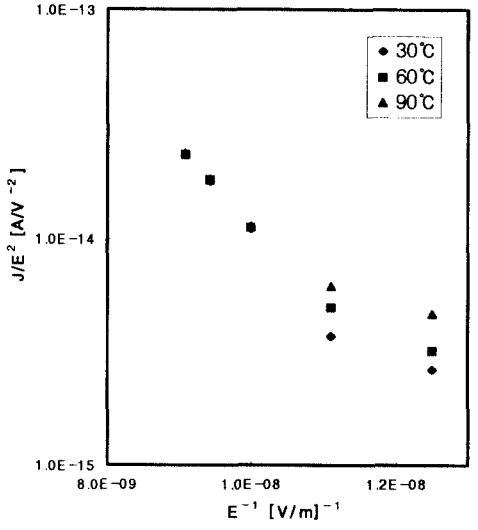

Fig. 13. Plot of the ln (J/E_{int}^2) and $1/E_{int}$ in the breakdown region.

(2) Current oscillation phenomena and their mobility

Fig. 14 shows the current-voltage oscillation phenomena of the specimen measured at 30℃. As shown in Fig. 14, it is known that

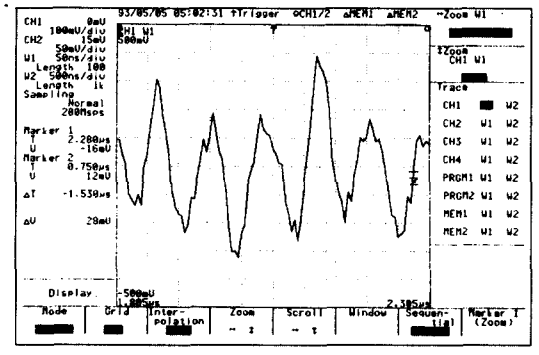

(a) Electric field 5×10^5[V/m]

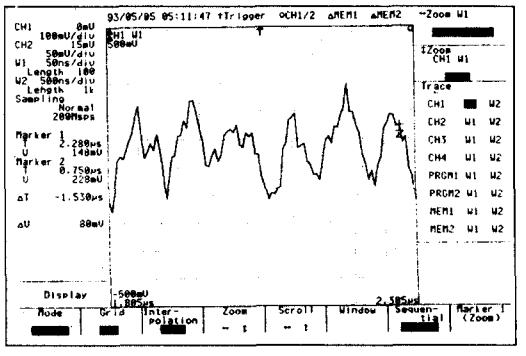

(b) Electric field 2×10^7[V/m]

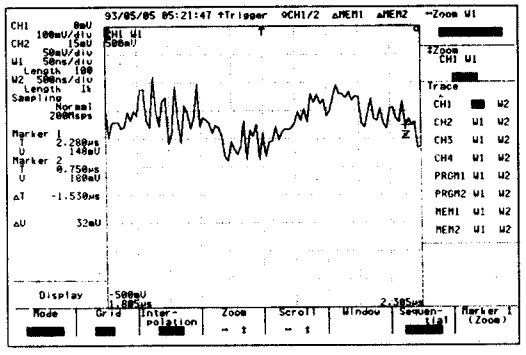

(c) Electric field 4×10^7[V/m]

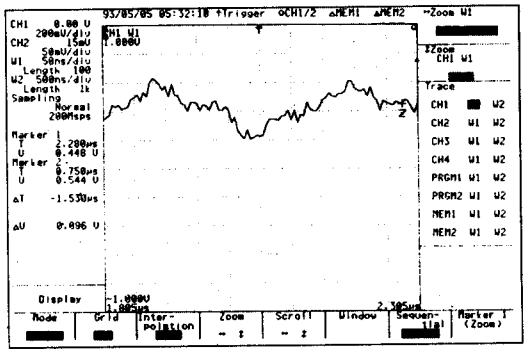

(d) Electric field 6×10^7[V/m]

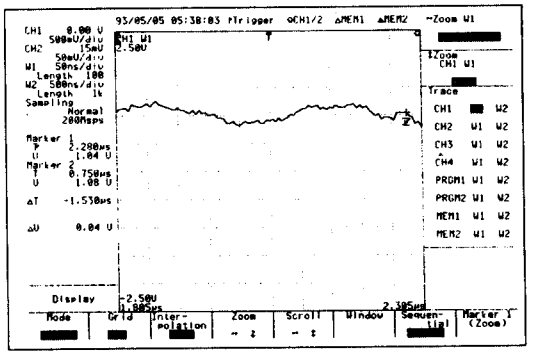

(e) Electric field 8×10^7[V/m]

Fig. 14. Current oscillation phenomena observed with osciloscope.

the oscillation amplitude of current decreases and the oscillation frequency increases, when the applied voltage increases from region Ⅰ of ohm region to region Ⅲ of breakdown region.

Fig. 15(a) is equivalent model considering intergranular layer between ZnO grain and ZnTi seed grain in microstructure of the specimen. In Fig. 15(b), r_g is a registance of ZnO grain, C_p and R_p is equivalent capacitance and registance of interface and depletion layer, respectively.

As for the most of injection electron in the electric field under breakdown region of varistor is filled in the trap level of intergranular layer, and then the injection electron does not influence on conduction, current is low in the low electrical field region. Also, part of the nontrapped injection electron which is accumulated in the intergranular layer has electrostatic force with the form of electron group. As increasing the electric field, the current oscillation phenomena is appeared with the junction nonequililrium of electrostatic force between intergrnular layer and depletion layer.

In the breakdown region, most of injected electron drift from conduction band in forward bias grain to conduction band in reverse bias grain without delay time, because the accumulative site of electron group does not exist in trap level of the intergranular layer as progressive accumulation of electron in the trap level[9].

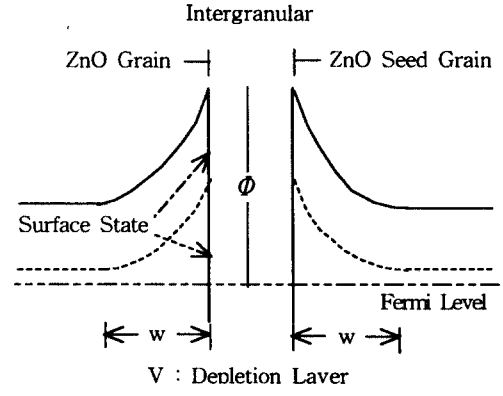

(a) Equivalant model in the intergranular layer

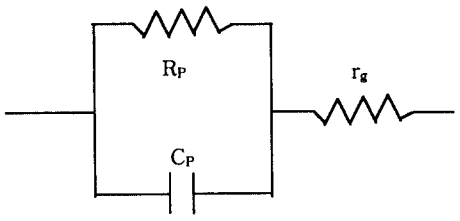

(b) Equivalant electrical model

Fig. 15. Equivalant model of ZnO varistors.

As the electron injected in forward bias is directed tunneling to reverse bias, current oscillation is hardly appeared in the electric field above breakdown region of varistor.

These phenomena are appeared in not only varistor but also in insulator and semiconductor. Paticularly, T. Yasukawa reported on the current oscillation phenomena in the conduction process of CdS[10].

The relation between carrier mobility(μ) and period(T) is calculated using the following equation.

$$\mu = \frac{d}{T \cdot E} [m^2/V \cdot s] \quad (10)$$

where, the thickness of intergrnular layer, d is 200Å, and E is the electric field intensity obtained in equivalent model. Carrier mobility will be calculated with sampling method from test results.

Fig. 14 shows the current oscillation phenomena in the various electric field of region Ⅰ, region Ⅱ and region Ⅲ, respectively. There are simultaneously group oscillation and irregular fine oscillation in these figures.

It is supposed that the origin of irregular fine oscillation is to drift a part of non-trapped injection electron from conduction band in forward bias grain to conduction band in reverse bias grain.

As shown in Fig. 16 (a)~(f), it is supposed that the injected electrons are accumulated in the intergranular layer on the effect of image charge, and then drift to the conduction band of reverse bias grain with increasing eletric field intensity[8].

These phenomena are the origin of group oscillation. Fig. 14 shows that the oscillation amplitude is proportional to the number of accumulated electron.

The amplitude of group oscillation in the low electric field intensity of region Ⅰ is larger than the irregular fine oscillation, but it is scarcely different in the high electric-field region Ⅲ.

As a result, the injected electrons in the breakdown region directly drift from conduction band in forward bias grain to conduction band in reverse bias grain, because the accumulative site of electron group does not exist in the trap level of the intergrnular layer as increasing the applied voltage.

Table 1 is shown the value of mobility obtained in each region using the equation (10). As shown in Table 1, the mobility of irregular fine oscillation is independent of electric field, but the mobility of group oscillation is smaller with increasing electric field intensity. Because of increased applied voltage, the number of accumulated group

Table 1. Mobility of carriers in the intergranular model

E_{int} [V/m]	5×10^5	1×10^7	2×10^7	3×10^7	4×10^7	5×10^7	6×10^7	7×10^7	8×10^7	1×10^8
Fine oscillation mobility [$m^2/V \cdot s$]	2.9×10^{-7}	1.6×10^{-8}	9×10^{-9}	7.1×10^{-9}	5.3×10^{-9}	3.2×10^{-9}	3×10^{-9}	3×10^{-9}	2×10^{-9}	1.6×10^{-9}
Group Oscillation mobility [$m^2/V \cdot s$]	4.9×10^{-8}	2.4×10^{-9}	1.1×10^{-9}	2.4×10^{-10}	1.7×10^{-10}	1.5×10^{-10}	1×10^{-10}	9.3×10^{-11}	8×10^{-11}	5.3×10^{-11}

electron is decreased due to the effect of image charge, and the characteristics of varistor will be appeared in sample for fastly distortion of junction, decreasing priode and amplitude due to the transportation of group electron.

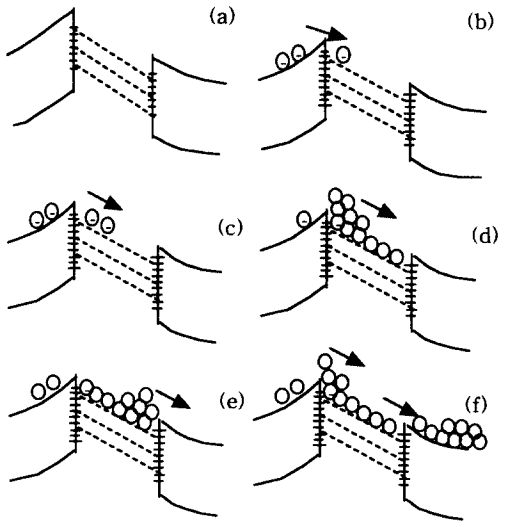

Fig. 16. The oscillation model of conduction in the intergranular layer.

4. CONCLUSIONS

The method making low-voltage ZnO varistors with the 3-composition seed grain of extra grain size was reported in this paper.

The results of the conduction mechanism and the oscillation characteristics of carrier for non-ohmic ZnO varistor fabricated by 3-composition seed grain method could be obtained as follows :

1. The knee voltage and nonlinear coefficient α of the specimen with 3-composition seed grain of 5 wt % are 5 V and 22, respectively.
2. The conduction mechanism is mainly governed by the thermoionic emission below the knee voltage but also the field emission of double Schottky model at above the knee voltage. The calculated activation energy and trap level of those region are 0.36 and 0.70 eV, respectively.
3. The conduction mechanism for the nonlinear region above the knee voltage can be analyzed by the Fowler-Nordheim tunneling effect. The barrier height of the model in this region is 0.26 eV.
4. The oscillation amplitude of carrier is inversely propotional to the applied voltage.
5. The mobility of irregular fine oscillation is $2.9\times10^{-4}m^2/V\cdot s$ at $5\times10^5V/m$ in this region, it is independent to the applied voltage.
6. The mobility of group oscillation is $4.9\times10^{-4}m^2/V\cdot s$ at $5\times10^5V/m$ in this region, it decreases with increasing applied voltage.

It is concluded that the method by three-composition seed grain would be better than any other methods, to make varistors with knee voltage below 5 $V_{(1mA/cm^2)}$. The conduction properties of ZnO varistor may be determinated by height of potential barrier. The characteristics of varistor will also be appeared with oscillation for the fast distortion of junction, decreasing the priode and the amplitude due to transportation of group electron.

REFERENCES

[1] Michio Matsuoka, Takeshi Masuyama and Yoshio Lida, "Nonlinear Electrical Properties of Zinc Oxide Ceramics", J. J. Appl. Phys., Proced. 1st Conference, Vol. (39) (1970).

[2] Kazuo Eda, Atsushi Iga and Michio Matsuoka, "Degradation Mechanism of Non-ohmic Zinc Oxide Ceramics", J. Appl. Phys., Vol. (51), No. 5, pp. 2678-2684(1980).

[3] Atsushi Iga, Michio Matsuoka and Takeshi

Masuyama, "Effect of Heat-Treatment on Current Creep Phenomena in Nonohmic ZnO Ceramics", J. J. Appl. Phys., Vol. (15), No. 9, pp. 1837-1848(1976).

[4] Kazuo Eda, Masanori Inada, Michio Matuoka, "Grain Growth Control in ZnO Varistors Using Seed Grains", J. Appl. Phys., Vol. (54), No. 2, pp. 1095-1099 (1983).

[5] R. C. Neville and C. A. Mead, "Tunneling Currents in Zinc Oxide", J. Appl. Phys., Vol. (41), No. 13, pp. 5285-5290(1970).

[6] T. K. Gupta, W. G. Carlson, "Barrier Voltage and Its Effect on Ability of ZnO Varistor", J. Appl. Phys., Vol. (53), No. 11, pp. 7401-7409(1982).

[7] Deltlev F. K. Hennings, Ruediger Hertung, Piet J. L. Reijnen, "Grain Size Control in Low Voltage Varistors", J. Am. Ceram. Soc., Vol. (73), No. 3, pp. 645-648(1990).

[8] L. M. Levinson and H. R. Philipp, "The Physics of Metal Oxide Varistors", J. Appl. Phys., Vol. (46), No. 3, pp. 1332-1341(1975).

[9] Kazuo Eda, "Transient Conduction Phenomena in Non-Ohmic Zinc Oxide Ceramics", J. Appl. Phys., Vol. (50), No. 6, pp. 4436-4442(1979).

[10] Takeshi Yasukawa, "Low-Frequency Oscillation in CdS Single Crystals", J. Appl. Phys., Vol. (37), No. 10, pp. 5285-5290 (1970).

[11] K. U. Jang, S. R. Kim, J. U. Lee, "Conduction Properties of ZnO Varistors Fabricated by 3-Composition Seed Grain", KIEEME(E), Vol. (2), No. 1, pp. 33-36 (1996).

[12] K. U. Jang, J. U. Lee, "Dielectric Properties of ZnO Varistor Fabricated by the Method of 3-Composition Seed Grain", KIEE, Spring Conference, pp. 69-72 (1992).